Topographic Variations in Normal Skin, as Viewed by *In Vivo* Reflectance Confocal Microscopy

Misbah Huzaira,* Francisca Rius,† Milind Rajadhyaksha,*‡ R. Rox Anderson,* and Salvador González*

*Wellman Laboratories of Photomedicine, Department of Dermatology, Massachusetts General Hospital, Harvard Medical School, Boston, Massachusetts, U.S.A.; †Biostatistics, Department of Preventive Medicine and Public Health, Faculty of Medicine, University of Málaga, Spain; ‡Lucid, Inc, Henrietta, New York, New York, U.S.A.

Near-infrared confocal microscopy is a new tool that provides skin images *in vivo*, with high resolution and contrast at a specific depth. Regional variations in live human skin viewed by confocal microscope have not been studied so far. *In vivo* reflectance confocal microscopy was performed in 10 adults (eight males, two females) of various skin phototypes. Six topographic sites were studied in each subject: forehead, cheek, inner and outer forearm surfaces, lower back and leg. Epidermal thickness at suprapapillary epidermal plates and rete pegs was measured during real-time imaging and the number and diameter of epidermal keratinocytes in each epidermal cell layer as well as the characteristics of dermal papillae were defined from the grabbed images. Stratum corneum appeared brighter in sun-exposed than in sun-protected areas and particularly pronounced in heavily pigmented individuals. The epidermal thickness at rete pegs, but not the suprapapillary epidermal plate, was greater in sun-exposed areas than in sun-protected sites except forearm flexor surface. The *en face* numerical density of granular keratinocytes is greater on the face as compared with all other sites, whereas the surface density of spinous keratinocytes is greater on sun-protected sites. Additionally, the number of basal keratinocytes per millimeter length of dermo-epidermal junction is greater in sun exposed areas. Interestingly, the dermal papillae shape varies and their sizes increase in circumference from sun-exposed to sun-protected sites, as observed at a specific depth below the stratum corneum. In summary, our results demonstrate that near infra-red reflectance confocal microscopy is a feasible tool for microscopic analysis of skin morphometry *in vivo*.

Key words: aging/dermis/stratum corneum. J Invest Dermatol 116:846–852, 2001

Histologic analysis of the topographic variations of normal skin is of relevance in dermatologic research. Several studies have been performed regarding the various parameters of normal skin, both from cadaveric skin as well as live healthy volunteers (Pinkus, 1951; Epstein and Maiback, 1965; Plewig, 1970; Bullough, 1972; Whitton and Everall, 1973; Holbrook and Odland, 1974; Bergstresser and Taylor, 1977; Bergstresser *et al*, 1978; Marks, 1981; Contet-Andonneau *et al*, 1999; Sanders *et al*, 1999), analyzing the biopsy samples after tissue processing and staining. Histologic processing induces artifacts and there is little information on the microscopic topography of normal skin. *In vivo*, near infrared reflectance confocal microscopy (CM) poses no tissue processing and is done in live skin, *in situ*.

Real-time reflectance CM operates by detecting single back scattered photons from the illuminated living tissue (Webb, 1996). A small pinhole in front of the detector allows to image with high resolution and contrast. The measured lateral resolution is 0.5–1 μm and the axial resolution (optical section thickness) is 3–5 μm (Rajadhyaksha *et al*, 1995, 1999), comparable with that of conventional histology. Contrast in confocal images is provided by refractive index differences of organelles and other microstructures from the background; melanin acts as a contrast agent in the pigmented epithelia (Rajadhyaksha *et al*, 1995; Dunn *et al*, 1996). With current technology, imaging is limited to a depth of 250–300 μm, which includes the entire epidermis, papillary dermis, and superficial reticular dermis. *In vivo* CM is painless, noninvasive, and does not harm the tissue; therefore, it can be performed as many times, on as many skin sites as required.

This study was designed to evaluate *in vivo* morphometric variations in normal human skin, at various topographical areas as viewed via CM. Our results demonstrate that CM is a feasible tool for morphometric analysis of skin *in vivo*.

Manuscript received September 19, 2000; revised December 27, 2000; accepted for publication January 26, 2001.

Reprint requests to: Dr. Salvador González, Assistant Professor of Dermatology, Wellman Laboratories of Photomedicine, 40 Blossom St. Bartlett Hall 814, Boston, MA 02114, U.S.A. Email: gonzalsa@helix.mgh.harvard.edu

Abbreviation: CM, near infra-red reflectance confocal microscope.

MATERIALS AND METHODS

Subjects investigated Ten healthy volunteers (eight males and two females) of various skin phototypes (four subjects of skin phototypes I–III and six of skin phototypes IV–VI) between the ages of 23 and 47 y were recruited in the study. All subjects had indoor occupations. Confocal imaging was done after obtaining informed consent on an Institutional Review Board approved protocol.

Sites investigated Six different skin sites were investigated in each subject. Each subject was imaged at similar locations in relation to anatomical landmarks. The sites were selected according to the availability to CM imaging and average daily sunlight exposure. These included three routinely sun-exposed (forehead, cheek, and forearm

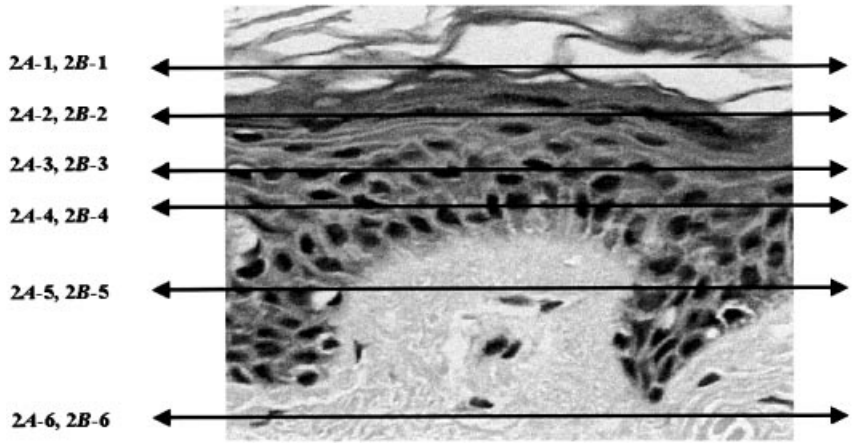

Figure 1. Vertical hematoxylin and eosin stained section of normal skin. The lines mark the approximate level of horizontal optical sectioning of various epidermal and dermal layers in **Fig 2**(***A***) (horizontal hematoxylin and eosin sections) and **Fig 2**(***B***) (optical sections as viewed by CM).

outer surface), and three routinely sun-protected sites (forearm inner surface, leg, and lower back).

Confocal imaging We used a commercially available CM (Vivascope 1000, Lucid Inc, Henrietta, NY). This microscope uses 830 nm diode laser operating at a power less than 30 mW at the tissue surface and a 30 × water immersion objective lens (refractive index of water = 1.33) of numerical aperture 0.9 NA. As previously reported (Rajadhyaksha *et al*, 1999), the best quality images are obtained by matching the refractive index of immersion medium with that of epidermis, ranging from 1.33 to 1.35.

Detailed description of the CM and optical parameters for *in vivo* imaging of human skin have also been previously reported (Rajadhyaksha *et al*, 1995, 1999). The skin was immobilized with a ring-template-fixture device that provides mechanical contact of the skin to CM. The ring-template was attached to the skin with a double sided sticking tape (Vasamedics, St Paul, MN; http://www.vasamedics.com).

In this CM system, a vertical (Z-axis) micrometer screw was used to adjust the depth of imaging (in μm); the horizontal (X–Y axis) micrometer screws were used to move the stage to image at a different spot at the same site so that one can ''fly'' through the skin. In our study, the field of view of the confocal images is 250 × 250 μm (680 pixels). We were able to view the skin to a depth of 200 μm.

Morphometric analysis In all imaged skin sites, the depths (in μm) of stratum corneum, various viable epidermal layers, suprapapillary epidermal plates and rete pegs were obtained during real-time imaging by reading the calibrated depth (Z-axis) micrometer. Descriptive features of stratum corneum in terms of brightness, presence of fissures or wrinkles, and hair shafts were also analyzed. Qualitative features were evaluated at a laser power of < 5mW in order to avoid back-scattered light saturation. The *en face* numerical density of granular and spinous keratinocytes (number of cells per *en face* mm^2) below the stratum corneum and their diameters were assessed from grabbed images. In doing so, 30–36 grabbed images were analyzed for each quantitative parameter.

The number of basal keratinocytes around each dermal papilla, at a specific depth below the stratum corneum, were counted to assess the number of basal keratinocytes per unit length of dermoepidermal junction. In doing that, the circumference of dermal papillae in a given image was measured by the following formula, which implies to the elliptical shapes (Eves, 1986):

$$k = 2\pi \{a^2 + b^2/2\}^{1/2}$$

where, a, b, and k correspond to smaller diameter, larger diameter, and circumference of the elliptical shapes, respectively.

In the dermis, starting approximately at a depth of 58–65 μm, we noted the extracellular matrix appearance and assessed the number of perfused blood vessels per unit area as well as their luminal diameters during real-time imaging.

Routine histology This study was not aimed to correlate the CM images with accompanying site histology; however, a single biopsy was obtained in one of the subjects from the forearm inner surface in order to help interpret standard CM images of normal skin.

Statistical methods Mean and standard deviation were calculated for each quantitatively assessed morphologic parameter. To compare parameters between body sites, a repeated measure of ANOVA test was used (Stevens, 1986) with one factor being the subject and another being the topographic area. A multiple comparison Bonferroni test was performed in order to detect those values among which there were significant differences ($p < 0.05$).

RESULTS

Gross interpretation of confocal features of normal skin (Figs 1 and 2*A*, *B*) Normal skin histology vertical and horizontal (*en face*) hematoxylin and eosin sections of stratum corneum, granular layer, and spinous compartment and dermo-epidermal junction are shown for comparison with CM images (**Figs 1** and **2*A***). **Figure 2**(***B***) illustrates a series of optically sliced (horizontal) confocal sections from live normal skin. The first image is that of a horizontal (*en face*) section of stratum corneum, with a roughened surface and fissures (**Fig 2*B*-1**), seen as a highly refractive layer due to a water/stratum corneum refractive index difference. The layer of granular keratinocytes (**Fig 2*B*-2**) lies underneath it. It is distinguished by the presence of large nuclei, that appear as dark areas and a thin rim of cytoplasm that appears bright and grainy. Grainy cytoplasm in CM images is due to organelles and other microstructures. The cellular compartment underneath is composed of spinous keratinocytes (**Fig 2*B*-3**) recognized by their cell size. In the horizontal plane, spinous keratinocytes are smaller than granular keratinocytes and adapt a honeycombed pattern. The central dark areas correspond to the nuclei surrounded by a bright margin of cell cytoplasm. In basal cells, confocal sections through the upper portion of cells show bright disks (**Fig 2*B*-4**). The disks always occur in supranuclear positions and are prominent in heavily pigmented skin individuals. As we increase the depth of penetration to image the deeper layers, we can see the dermal papillae, centered by blood vessels and blood cells tumbling on top of each other, during real time imaging, outlined by basal keratinocytes (**Fig 2*B*-5**). The basal keratinocytes appear brighter than the surrounding spinous keratinocytes. Below the dermoepidermal junction, a network of collagen and elastin fibers of diameter 1–5 μm and bundles of diameter 5–25 μm can be seen within the papillary dermis and upper dermis, having dark spaces in between, corresponding to the spaces in the fibers themselves (**Fig 2*B*-6**).

Analysis of topographic variations – qualitative analysis

Stratum corneum The stratum corneum appears much brighter in darker skin individuals and on sun-exposed sites. The brightness measured in the same subject using same laser power at a sun-protected site, is significantly lower than at sun-exposed sites (**Fig 3*A***). The stratum corneum was fissured and wrinkled in the sun-exposed areas mainly on the face, when compared with sun-protected sites (**Fig 3*B***). Hair shafts were more frequently seen on cheek and forehead than in any of the remaining sites.

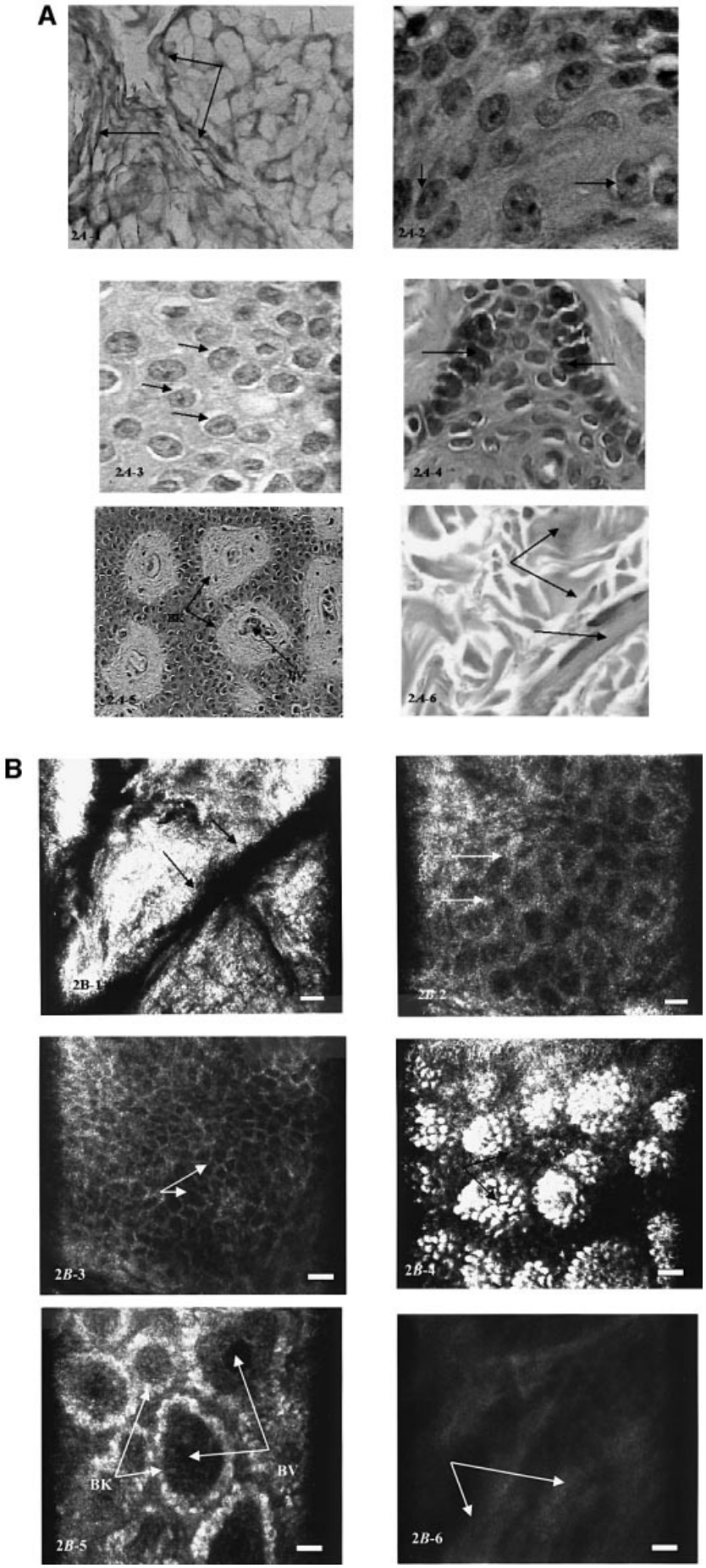

Figure 2. Correlation of en face routine histologic images and *in vivo* CM images (*A*) *En face* hematoxylin and eosin stained sections of normal skin. Stratum corneum, showing the presence of fissures on the surface (*A-1*, *arrows*). The granular keratinocytes (*A-2*, *arrows*) have larger nuclei as compared with smaller sized nuclei of spinous keratinocytes (*A-3*, *arrows*). The melanin-containing basal keratinocytes (*A-4*) are found at the level of suprapapillary epidermal plate (*arrows*). The dermal papillae (*A-5*) surrounded by basal keratinocytes (BK, *arrows*) and are centered by blood vessels (BV, *arrows*) and basal keratinocytes and surrounding them. Collagen fibers and bundles (*A-6*, *arrows*) are also seen. (*B*) *In vivo* CM images of forearm outer surface (skin phototype V). Note the fissured (*arrows*) appearance of stratum corneum (*B-1*). The granular cell layer is composed of keratinocytes with larger nuclei (*arrows*) and grainy appearance of cytoplasm (*B-2*). The spinous keratinocytes (*B-3*) have smaller sized nuclei. Highly refractile structures between spinous keratinocytes, that may correspond to melanin, are also pointed out (*arrows*). The ''melanin hats'' are also seen (*B-4*, *arrows*), located above the basal keratinocytes at suprapapillary epidermal plate (*B-5*). The collagen fibers and bundles are also seen (*B-6*, *arrows*). *Scale bar*: 25 μm.

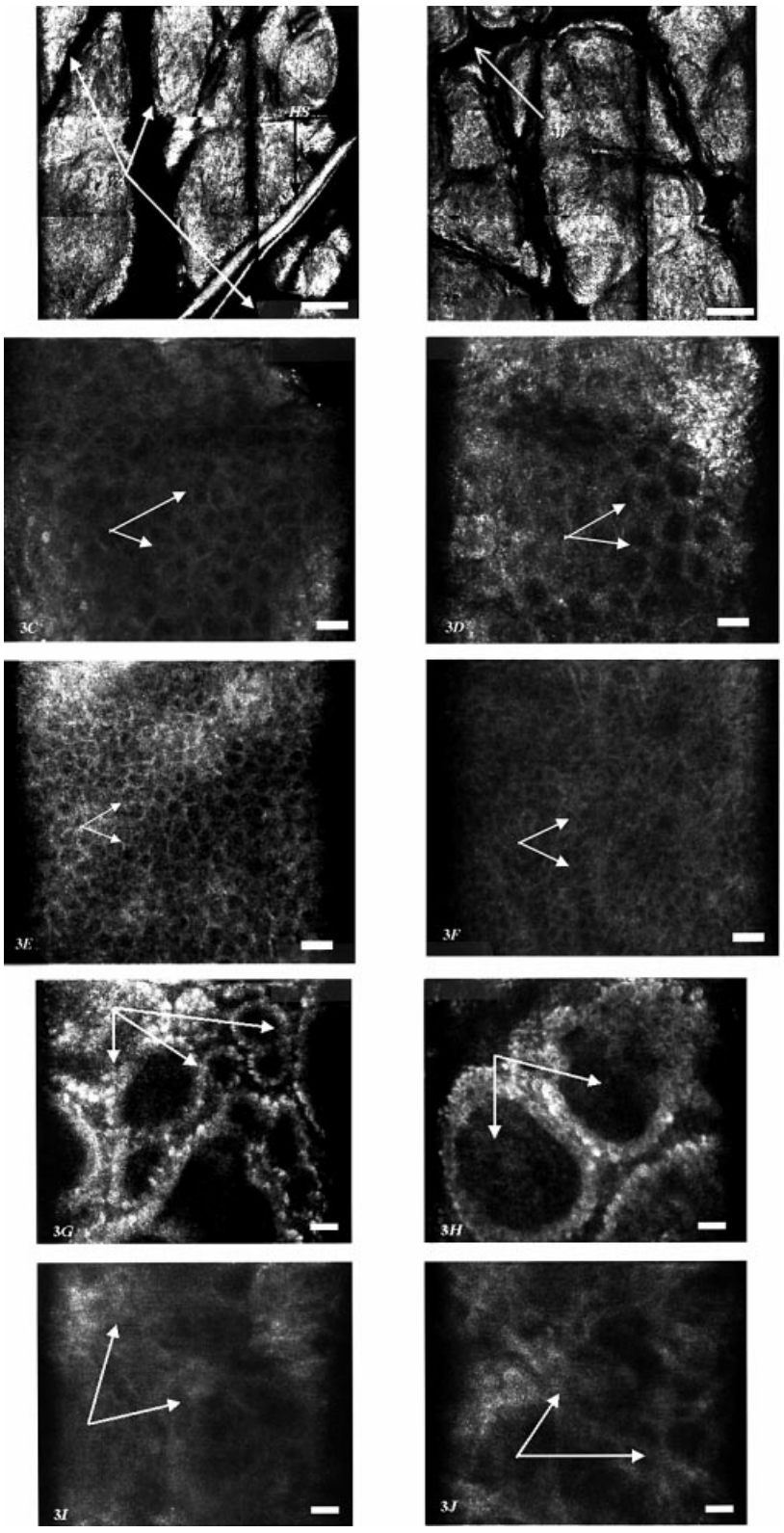

Figure 3. Comparison between *in vivo* CM images obtained from sun-exposed sites and sun-protected sites. Maps of stratum corneum over an area of 750 × 600 μm, illustrating differences in morphology of wrinkles (W, *arrows*) and more frequently encountered hair shafts (HS, *arrows*) on the stratum corneum of sun-exposed sites (*A*) as compared with sun-protected sites (*B*) The number of granular keratinocytes (*arrows*) is greater on sun-exposed sites (*C,D*), whereas the number of spinous keratinocytes (*arrows*) are more on sun-protected sites (*E,F*). Of note is the morphology and number of dermal papillae (*arrows*) at sun-exposed (*G*) and sun-protected sites (*H*) and the number of dermal papillae on both sides. Also note that the collagen is seen (*arrows*) as arranged in the form of clumps of bundles on sun-exposed sites (*I*) as compared with fibers on sun-protected sites (*J*). *Scale bars:* (*A*, *B*) 100 μm; (*C–J*) 25 μm.

En face* section of dermal papillae** At an average depth of 58–65 μm, the shape and circumference of the dermal papillae varies significantly from sun-exposed to sun-protected sites. In sun-exposed areas, they are randomly arranged, more numerous, and irregularly shaped (**Fig 3*G*).** In sun-protected sites, they appear distributed in a smooth fashion, fewer in number, and regularly ellipse shaped (**Fig 3*H). The circumference of the dermal papillae are significantly larger on the protected sites than on the areas of chronic sun exposure and wear and tear.

Collagen Images analyzed from the papillary and upper reticular dermis from sun-exposed sites reveal a network of voluminous mushy bundles (**Fig 3*I***), whereas in sun-protected sites it is fine, smooth, and contains elongated fibers (**Fig 3*J*).**

Analysis of topographic variations – quantitative analysis

Number of granular and spinous keratinocytes per unit area The *en-face* numerical density of granular keratinocytes is maximum on the face (forehead and cheek), as compared with the back, where the

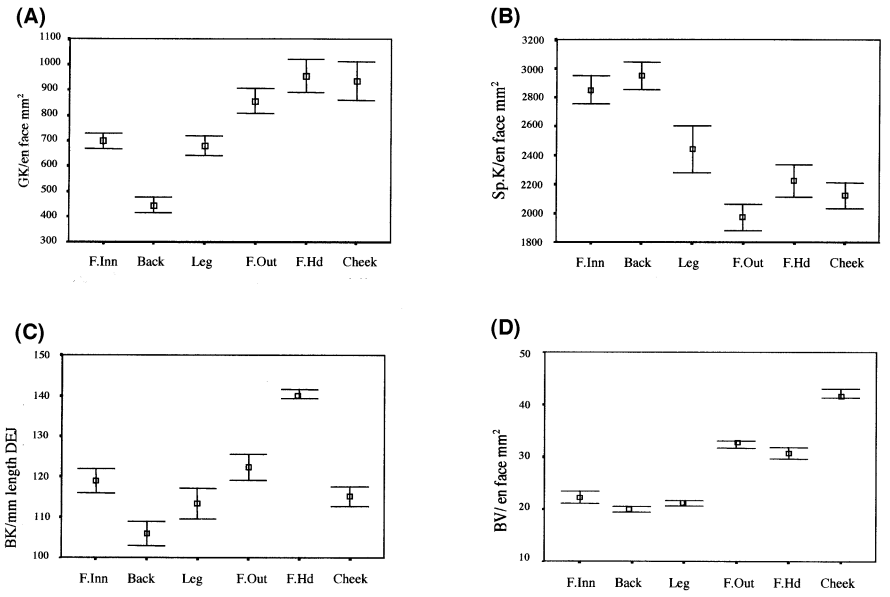

Figure 4. Topographic variations in the numerical density of several histological parameters. Graphic representation of number of granular (*A*), spinous (*B*) and basal keratinocytes (*C*), and perfused blood vessels (*D*) as viewed by CM. Bars correspond to 95% confidence interval from the mean. GK, granular keratinocytes; Sp.K, spinous keratinocytes; BK, basal keratinocytes; BV, basal vessels.

Table I. Topographic variations in the thicknesses of various epidermal keratinocyte layers (see text for details)

	Stratum corneum			Stratum granulosum			Suprapapillary plate			Depth of rete pegs		
Areas	No.	mean	SD	No.	mean	SD	No.	mean	SD	No.	mean	SD
F. Inn	36	9.58	0.8	36	13.13	3.3	36	50.83	3.57	36	130.36	26.05
Back	36	10.41	0.8	36	11.41	4.0	36	62.05	3.88	36	101.58	8.54
Leg	36	8.08	1.8	36	14.36	4.4	36	65.44	4.86	36	110.58	8.87
F. Out[a]	36	12.96	2.3	36	7.07	3.0	36	58.47	5.66	36	134.55	17.8
F. Hd	36	13.66	2.9	36	6.27	3.3	36	63.71	3.6	36	130.25	10.55
Cheek	36	12.05	1.7	36	7.36	2.7	36	60.25	3.99	36	115.25	12.9

[a]F. Out, outer forearm; F. Hd, forehead.

number is significantly lower. The number of granular keratinocytes is significantly higher in sun-exposed areas as compared with sun-protected sites ($p < 0.0001$) (**Fig 4*A*). Figure 3**(***C*, *D*) also illustrate this difference. The diameter of granular keratinocytes is 25–35 μm.

The number of spinous keratinocytes, on the contrary is greater on the sun-protected sites. Their average count is significantly greater on the back and forearm inner surface as compared with sun-exposed areas ($p < 0.0001$). **Figures 4**(***B***) and (***E***, ***F***) illustrate this discrepancy between the epidermis on the cheek and back, respectively. The diameter of spinous keratinocytes ranges from 15 to 25 μm.

Number of basal keratinocytes per unit length of dermoepidermal junction The greatest number of basal keratinocytes per millimeter of dermoepidermal junction is found on the forehead, whereas the lowest value was observed on the back ($p < 0.0001$) (**Fig 4*C***). The number of basal keratinocytes did not vary significantly among different sun-exposed or sun-protected sites. The diameter of basal keratinocytes is found to be 7–12 μm.

***En face* numerical density of perfused blood vessels at a depth of 58–65 μm** The number of blood vessels is found to be significantly greater on sun-exposed areas, especially on the forearm outer surface and cheek (**Fig 4*D*).**

Layer thicknesses As expected, the stratum corneum is significantly thicker in the sun-exposed areas ($p < 0.0001$), especially in the forehead (**Table I**). The stratum granulosum is significantly thicker in the sun-protected than in the sun-exposed sites. These latter sites show a greater variability (**Table I**).

Suprapapillary epidermal plate is significantly thinner on the forearm inner surface than on the remaining sites ($p < 0.0001$). At rete peg depth, the thickness of epidermis varies from sun-exposed to sun-protected sites, being significantly greater in sun-exposed than on sun-protected sites (**Table I**).

Capillary loops On the areas of chronic sun exposure, at a depth of 58–65 μm capillary loops are of smaller diameter (3–5 μm), more numerous, and grouped together in small clusters. On the sun-protected sites, capillaries are larger in diameter (4–10 μm), fewer in number, and arranged as isolated loops.

DISCUSSION

CM is a new noninvasive, high resolution imaging tool, and is being used to study a variety of commonly encountered skin conditions (Gonzalez *et al*, 1999a–d; Aghassi *et al*, 2000). CM images should, however, be interpreted on the basis of a thorough knowledge of normal skin morphometric variation. In this study, we report the use of CM to analyze several morphometric parameters, comparing various topographic sites (forearm inner and outer surface, forehead, cheek, leg, and lower back).

Qualitative analysis The description of the parameters analyzed qualitatively relies on the following characteristics: (i) the appearance of stratum corneum, being brighter and roughened on primarily sun-exposed sites; (ii) the presence of ''melanin hats'' on top of basal keratinocytes, especially on sun-exposed sites and in darkly pigmented individuals; (iii) the dermoepidermal junction being rather flat; and (iv) collagen appearing as a dense network of fibers and bundles on the lumbar back.

The fact that stratum corneum, as seen by CM is brighter (Rajadhyaksha *et al*, 1995), roughened, and wrinkled on the areas of chronic sun exposure, may be partly due to the skin's adaptability response to daily stresses. Furthermore, in the basal cell layer we have stated the presence of very bright disks, which are particularly prominent in darkly pigmented skin. With the background knowledge of melanin serving as the best endogenous contrast agent (Rajadhyaksha *et al*, 1995, 1999), the brightness and supranuclear position of these disks suggests that these may be the protective ''melanin hats'' located above the nuclei. These disks are not as obvious in lightly pigmented skin individuals.

The *en-face* morphology of the dermoepidermal junction is different on the face and back than on other analyzed sites. They are numerous, irregularly shaped, and randomly arranged on the face, suggestive of mild papillomatosis. On the other hand, the dermoepidermal junction is rather flat on the lower back. Whether chronic sun exposure plays a part in affecting the undulations of the basement membrane or not, remains unclear.

In the dermis, we have found some morphologic differences of the collagen at sites of chronic sun exposure, when compared with normally protected sites. It is irregular, compressed with a haphazard arrangement of voluminous bundles as seen through CM in areas of chronic sun exposure. Also, collagen bundles seem to be more obscure on sun-exposed than on sun-protected sites, perhaps due to increased melanin pigmentation that interferes with light transmission (Rajadhyaksha *et al*, 1995, 1999). It is not possible, however, to state whether these fibers also contain elastin tissue in addition to collagen, when visualized by CM.

Quantitative analysis The main findings are: (i) the *en face* numerical density of granular keratinocytes is greater on sun-exposed sites, whereas the *en face* numerical density of spinous keratinocytes is more on sun-protected sites; (ii) the number of basal keratinocytes per millimeter of dermoepidermal junction and the numerical density of blood vessels is greater on sun-exposed sites; (iii) the stratum corneum is considerably thicker on sun-exposed areas; and (iv) the rete pegs are significantly elongated in forearm and facial skin.

The number of epidermal keratinocytes per unit area and their diameters have been previously analyzed *in vivo* by tandem scanning CM (Corcuff and Leveque, 1993). Our results do not correlate with their data. They limited the study to forearm and wrist and no information regarding their number on individual sites and range of standard deviation is available.

As evident from our results, the *en face* number of granular keratinocytes is greater in the sun-exposed sites than in routinely sun-protected sites (**Fig 3*C*, *D*).** On the contrary, the number of spinous keratinocytes is greater in sun-protected sites than in chronically sun-exposed sites (**Fig 3*E*, *F*).** One possible explanation for this finding might be the disproportion in epidermal cell turn over and the rate of exfoliation from the surface, as the sun-protected sites are not routinely subjected to sheer stresses of daily routine (Mackenzie, 1975).

Variations in normal skin related to age and gender have been reported (Whitton and Everall, 1973). It has also been observed that the degree of variability on the normally clothed body sites is less than that on the normally unclothed sites. This supports our results that the epidermal dimensions are affected to some extent by environmental factors, and it also agrees with the observations reported by of other investigators (Freeman *et al*, 1962); however, other factors may also be involved (Whitton and Everall, 1973). We herein report that the number of basal keratinocytes per unit length of dermoepidermal junction can be assessed by *in vivo* CM. We have found that their number is greater in forehead and cheek, than at other sites being examined.

Epidermal thickness is of considerable significance in dermatologic research. Our results have shown that thickness of epidermis varies significantly at different skin sites. A considerable amount of work has been done and reported regarding the thickness of epidermis, both *in vivo* (Hulsbergen Henninng, 1977; New *et al*, 1991; Corcuff *et al*, 1993; Corcuff and Leveque, 1993) and *ex vivo* from biopsy samples (Kligman, 1964; Whitton and Everall, 1973; Holbrook and Odland, 1974) defining the values of epidermal thickness on different sites.

Concerning stratum corneum, our results show that it is thinner on sun-protected sites (Klein-Szanto, 1977). Corrections, for the effects of hydration status on the thickness of stratum corneum during real-time CM imaging are not studied in this work. Previous data (Whitton and Everall, 1973) also states that the thickness of living epidermis at the suprapapillary epidermal plate is greater on leg and back (74 μm and 55 μm, respectively) as compared with other sites. We have analyzed the thickness of the suprapapillary epidermal plate and the depth of rete pegs, as two separate entities and the values obtained by *in vivo* CM are in close proximity to those previously defined. We have been able to show statistically significant differences on the sites that were analyzed (**Table I**). The depth of rete pegs is considerably less on the sun-protected sites with the exception of the forearm inner surface where it is found to be approximately 130 μm. A lower number of dermal papillae per horizontal (*en face*) unit area might be responsible for this greater value.

Although our study supports the feasibility of *in vivo* confocal microscopy imaging to evaluate human skin morphometry, it has certain limitations: (i) *in vivo* morphometric analysis of skin is performed based upon *en face* CM images (for a better correlation to conventional skin histology we used vertical sections); (ii) we are yet not able to define the cellular organelles and nuclear details as viewed with the currently available system; and (iii) the maximum depth of dermis as seen by *in vivo* CM is not sufficient to analyze the skin appendages, such as hair follicles, sebaceous glands, etc.

CONCLUSIONS

In summary, this study highlights the normal skin morphometric variations using near-infrared reflectance CM *in vivo*. Our results show statistically significant differences of normal skin topographic morphology. Epidermal cell population, thicknesses of various epidermal layers, morphology of dermoepidermal junction, dermal collagen, and vasculature vary significantly from areas of average daily sun exposure to routinely sun-protected sites. The use of noninvasive imaging technique to analyze epidermal and dermal features, including dermal microvasculature may benefit research in dermatology.

This work was partially supported by Lucid, Inc.

REFERENCES

Aghassi D, Anderson RR, Gonzalez S: Confocal laser microscopic imaging of actinic keratoses *in vivo*: a preliminary report. *J Am Acad Dermatol* 43:42–48, 2000

Bergstresser PR, Taylor JR: Epidermal ''turnover-time''—a new examination. *Br J Dermatol* 96:503–506, 1977

Bergstresser PR, Praiser RJ, Taylor JR: Counting and sizing of epidermal cells in normal human skin. *J Invest Dermatol* 70:280–284, 1978

Bullough WS: The control of epidermal thickness. *Br J Dermatol* 87:187–199, 347–354, 1972

Contet-Andonneau JL, Jeanmaire C, Pauly G: A histological study of human wrinkle structures: a comparison between sun exposed areas of the face, with or without wrinkles and sun protected areas. *Br J Dermatol* 140:1038–1047, 1999

Corcuff P, Leveque JL: *In vivo* vision of the human skin with Tandem Scanning Microscope. *Dermatology* 186:50–54, 1993

Corcuff P, Bertrand C, Leveque JL: Morphometry of human epidermis *in vivo* by real-time confocal microscopy. *Arch Dermatol Res* 285:475–481, 1993

Dunn AK, Smithpeter C, Welch AJ, Richard-Kortum R: Sources of contrast in confocal reflectance imaging. *Appl Opt* 35:3441–3446, 1996

Epstein WL, Maiback HI: Cell renewal in human epidermis. *Arch Dermatol* 92:462–468, 1965

Eves H: Mensuration formulas. In: Beyer WH (ed.). *Standard Mathematical Tables*. Boca Raton, FL: CRC Press, 1986, pp 121–133

Freeman LG, Cockerall EG, Armstrong J, Knox JM: Sunlight influencing the thickness of epidermis. *J Invest Dermatol* 39:295–298, 1962

Gonzalez S, Gonzalez E, White WM, Rajadhyaksha M, Anderson RR: Allergic Contact Dermatitis. Correlation of *in vivo* confocal imaging to routine histology. *J Am Acad Dermatol* 40:708–713, 1999a

Gonzalez S, Rajadhyaksha M, Gonzalez-Serva A, White WM, Anderson RR: Confocal reflectance imaging of folliculitis *in vivo*; correlation with routine histology. *J Cut Pathol* 26:201–205, 1999b

Gonzalez S, Rajadhyaksha M, Rubinstein G, Anderson RR: Characterization of Psoriasis in vivo by reflectance confocal microscopy. *J Med* 30(5&6):337–356, 1999c

Gonzalez S, Rubinstein G, Mordovtseva V, Rajadhyaksha M, Anderson RR: *In vivo* abnormal keratinization in Darier-White's disease as viewed by real-time confocal imaging. *J Cut Pathol* 26:504–508, 1999d

Holbrook KA, Odland GF: Regional differences in the thickness (cell layers) of the human stratum corneum: An ultra structural analysis. *J Invest Dermatol* 62:415–422, 1974

Hulsberger Henning JP, Beerens EGJ, Vander Leun JC: A non-invasive method for measuring epidermal thickness, *in vivo*. *Arch Dermatol Res* 258:25–32, 1977

Klein-Szanto AJP: Stereologic baseline data of normal human epidermis. *J Invest Dermatol* 68:73–78, 1977

Kligman AM: The biology of stratum corneum. In: Montagne W, Lobitz WC (eds). *The Epidermis*. New York: Academic Press, 1964, pp 407–408

Mackenzie IC: Ordered structure of epidermis. *J Invest Dermatol* 65:45–51, 1975

Marks R: Measurement of biological aging in human epidermis. *Br J Dermatol* 104:627–633, 1981

New KC, Petroll WM, Boyde A, et al: *In vivo* imaging of human teeth and skin using real-time confocal microscopy. *Scanning* 13:369–372, 1991

Pinkus H: Examination of the epidermis by strip method of removing horny layers. Observations on thickness of horny layer and on mitotic activity after stripping. *J Invest Dermatol* 16:383–386, 1951

Plewig G: Regional differences of cell sizes in human stratum corneum. *J Invest Dermatol* 54:19–23, 1970

Rajadhyaksha M, Grossman M, Esterowitz D, Webb RH, Anderson RR: *In vivo* confocal scanning laser microscopy of human skin: Melanin provides a good contrast. *J Invest Dermatol* 104:946–952, 1995

Rajadhyaksha M, Gonzalez S, Zavislan J, Anderson RR, Webb RH: *In vivo* confocal scanning laser microscopy of human skin II. Advances in instrumentation and comparison to histology. *J Invest Dermatol* 113:293–303, 1999

Sanders JE, Goldstein BS, Leotta DF, Richards KA: Image processing techniques for quantitative analysis of skin structures. *Comput Methods Prog Biomed* 59:167–180, 1999

Stevens J: Repeated measure analysis. In: Stevens J (ed.). *Applied Multivariate Statistics for the Social Sciences*. Hillsdale, NJ: Lawrence Erlbaum Associates, 1986, pp 402–441

Webb RH: Confocal optical microscopy. *Rep Prog Phys* 59:427–471, 1996

Whitton JT, Everall JD: The thickness of epidermis. *Br J Dermatol* 89:467–476, 1973